D.A. Sant *et al.*, *Man and Environment* XXXI(2): 9-20 [2006].

Flood Plain Record of the Southwest Indian Monsoon During the Last Glacial

Dhananjay A. Sant, Govindan Rangarajan[1], K. Krishnan[2], N. Basavaiah[3], Chintan Pandya, Mitesh Sharma and Yogi Trivedi

Department of Geology
The Maharaja Sayajirao
University of Baroda,
Vadodara 390002

1 Centre for Theoretical Studies and Department of Mathematics, Indian Institute of Science, Bangalore

2 Department of Archaeology and Ancient History, The Maharaja Sayajirao University of Baroda, Vadodara 390 002

3 Indian Institute of Geomagnetism, Mumbai

Abstract

Rapid oscillations in the intensity of the Southwest Indian monsoon during the last glacial phase have been inferred for the first time, from newly generated continental records from the site of Bhimpura, located in the Mahi river flood plain in the tropical semi-arid parts of western India. The flood plain sediment belonging to the Last Glacial is characterized using grain size, degree of sorting, sediment facies, magnetic susceptibility, carbonate percentages (calcrete, $CaCO_3$ and calcite), opaque magnetic heavy minerals, common rock forming minerals, and clay mineral percentages. Synthesizing these climate sensitive variables, seven flood periods and non-flood periods are identified. These episodes reflect strong and weak monsoonal phases at a time scale of a few thousand years.

Introduction

The major climatic system influencing South Asia is the Southwest Indian Monsoon (SwIM), which controls the agricultural economy of this region. The long term dynamics of SwIM are understood by analysing sediment cores from different parts of the Indian ocean, Arabian sea and Bay of Bengal (Gupta and Thomas 2003; Altabet *et al.* 2002; Thamban *et al.* 2001; Sarkar *et al.* 2000; Leuschner and Sirocko 2000; Schulz *et al.* 1998; Colin *et al.* 1998; Wang *et al.* 1999; Overpeck *et al.* 1996; Sirocko *et al.* 1993). It is known that the release of heat over the Qinghai-Tibetan Plateau drives the SwIM towards the continent (Overpeck *et al.* 1996; Thompson *et al.* 1997). Rangarajan and Sant (2000) reasoned that the Arabian Sea sediments are influenced by the influx of melt water from the Himalayas. Further, Sant and Rangarajan (2002), using marine and ice core records from around the world, rationalized leads and lags for the onset of a climate change, including change in the SwIM.

A network of streams sculpture the continent. Both small and large drainage systems respond to climate change in terms of change in sediment character. Studies on continental sediments have led to an understanding of the response of continents to climate change (for China: Porter 2001; Xiao *et al.* 1995; Porter and An 1995, Kohfeld 2001, for Africa-Madagascar: Gasse and Van Campo 1998; Bonnefille and Charlie 2000; and for India: Singh 2004; Sinha *et al.* 2004; Kale *et al.* 2004; Juyal, *et al.* 2004; Sant *et al.* 2004; Jain and Tandon 2003; Juyal *et al.* 2003; Mishra and Rajaguru 2001; Srivastava *et al.* 2001; Juyal *et al.* 2000; Khadkikar *et al.* 1999; Tandon *et al.* 1997; Enzel *et al.* 1999; Andrews *et al.* 1998; Kotlia *et al.* 1997; Wasson *et al.* 1983). Studies of fluvial environments in the world's hyper-arid, arid, semi-arid and dry-sub-humid regions have shown that fluvial sediments in combination with aeolian and lacustrine deposits along with pedogenic and digenetic features, have a high potential for palaeoenvironmental reconstruction (Xiao *et al.* 1995; Knox 2000; Castelltort and Driessche 2003 and references cited therein). Studies in these regions have shown that fluvial deposits have survived subsequent reworking and are preserved as sedimentary successions (Merifield 1987; Reid 1994; Reid and Frostick 1997; Nanson and Tooth 1999 as cited in Tooth 2000). Regional to global level climatic signatures are often well preserved within flood plain sediments (Macklin and Lewin 2003).

In case of monsoonal rivers, where rainfall is seasonal and the region is tectonically stable, the drainage basin response can be attributed largely to a single variable, "the climate". Irrespective of climatic zones and geomorphic setup, major and minor rivers across the Indian subcontinent show a thick sequence of sediment, deposited within the river channel. This further exemplifies the response of streams with respect to regional-global climate. Therefore, characterization of flood plain sediments enables understanding of changes in processes and their intensities. Climate sensitive proxy records as determined from flood plain sediments, facilitates appraisal of climate variability and change. The SwIM has played a crucial role in the deposition of flood plain sediments in the Indian subcontinent (Khadkikar *et al.* 1999; Juyal *et al.* 2000; Srivastava *et al.* 2001; Jain and Tandon 2003; Juyal *et al.* 2004; Sant *et al.* 2004). Therefore, the flood plain sediments preserve the signature of formative processes and thereby record changes in the intensity of the SwIM in response to global climate change. This paper attempts to identify the signatures of the SwIM in terms of flood episodes. In order to understand the regional and global significance, continental data has been generated from Bhimpura (22° 19' 08.58" N; 73°05' 00.97" E, 33.3 m AMSL), from the Mahi flood plain, southern Cambay Alluvial Plain (CAP), tropical western India.

Previous studies undertaken in and around the Mahi and Sabarmati river basins have led to significant progress in understanding various features of Quaternary sediments. These include studies pertaining to stratigraphy and depositional environment (Pant and Chamyal 1990; Merh and Chamyal 1997; Tandon *et al.* 1997; Malik *et al.* 1999; Jain and Tandon 2003); palaeoclimatic reconstructions (Wasson *et al.* 1983; Tandon *et al.* 1997; Khadkikar *et al.* 1999; Juyal *et al.* 2000; Srivastava *et al.* 2001); the role of man in the region (Zeuner 1950; Subbarao 1952; Allchin and Goudie 1971; Allchin *et al.* 1978); and chronology using the thermoluminescence method (Tandon *et al.* 1997; Juyal *et al.* 2000; Srivastava *et al.* 2001; Juyal *et al.* 2003; Juyal *et al.* 2004). In addition to this, some earlier workers have compared sediment units and their chronology within and across the Mahi and Sabarmati alluvial basins (Pant and Chamyal 1990; Chamyal and Merh 1992; Tandon *et al.* 1997; Khadkikar *et al.* 1999; Malik *et al.* 1999; Juyal *et al.* 2000; Srivastava *et al.* 2001; Jain and Tandon 2003).

However, till date, no attempt has been made to characterize flood plain sediment and quantify changes in allogenic and authigenic records through time. Therefore, the present study aims at characterizing continental sediments, analyzing changes in physical and statistical parameters, identifying episodes within broad climatic phase (the Last Glacial), and providing detailed information on temporal (short-term) changes in climate sensitive proxies, in addition to understanding its global status.

Methods of Study

The site of Bhimpura and the Mahi flood plain forms a part of the CAP, a vast stretch of flat land with a mean elevation of 40 m AMSL, spread over the Cambay rift zone between Saurashtra and the Aravalli uplands. The palaeo-Sabarmati, palaeo-Mahi, palaeo-Dhadar and palaeo-Narmada are the important rivers responsible for building up the CAP (Sant and Karanth 1993). The incised flood plain and flood plain dunes within the Mahi and Sabarmati basin structure the topographic expression over the CAP. Geomorphologically the site falls along the eastern bank of the southwestern edge of Mahi flood plain which flows into the Gulf of Cambay (Fig. 1).

The representative samples were collected at 15 cm intervals from a 1513 cm open step-trench at Bhimpura, following recording of sedimentary structures, nature of pedogenesis and other related observable features. A total of 102 samples were collected from this section. In the present paper, proxy records from depths of 433 to 1513 cm are discussed. Granulometric analysis was performed by dry sieving 100 g of bulk sample. Fourteen sieve fractions namely, 420 μm, 250 μm, 210 μm, 149 μm, 125 μm, 106 μm, 90 μm, 75 μm, 63 μm, 53 μm, 45 μm, 37 μm, 25 μm and <25 μm were used. Magnetic susceptibility was measured for bulk sediments using Bartington MS2 Magnetic Susceptibility Meter at two frequencies (0.47 kHz and 4.7 kHz). The low frequency mass susceptibility (χ_{LF} bulk) and frequency dependent magnetic susceptibility (χ_{FD}(%)bulk) were calculated. Frequency dependent magnetic susceptibility was calculated as percentages from the ratio of difference between mass magnetic susceptibility at two frequencies and the low frequency susceptibility. The results are represented as magnetic susceptibility (χ_{LF})bulk and χ_{FD}(%)bulk. Carbonate concentration in the sediment is determined by treating <25 μm grain size fraction with 1N HCL, determining calcrete percentage from bulk 100 gm of sample 420 μm and 250 μm size sieve fractions and quantifying percentage of calcite mineral from X-ray diffractogram using base line fit method. Similarly, other minerals namely, quartz, feldspars, calcites, smectite, chlorite, illite, and hematite were also quantified. Mineralogy was determined by analyzing <25 μm size bulk sample on Philips PW1840 X ray diffraction (Cu Kα source (λ = 1.5418); by scanning between 2Φ ranging from 3° to 40° with a scanning speed of 0.02° per second). Opaque magnetic heavy mineral percentages were calculated for all samples after separation of magnetic minerals using hand magnet from 10 gm of bulk sample. These are evaluated to see their sensitivity to a climate change regionally and globally.

Results and Discussion

Grain size and Sediment facies records

The flood plain sequence at Bhimpura shows trough cross-bedded gravel and sand at the base (1513 to 1203 cm) followed by visually massive unstratified sandy-silty facies (1203 to 433 cm). The sieve fractions from 420 μm and 250 μm yielded calcrete from depths of 433 to 1203 cm whereas, the same sieve fractions from depth 1503 to 1203 cm, yielded medium to coarse sand and gravel. Further sieve fractions at 210 μm, 149 μm and 125 μm together are grouped as fine sand; 106 μm, 90 μm and 75 μm, as very fine sand; and 63 μm, 53 μm, 45 μm, 37 μm, 25 μm and <25 μm as silt (Folk 1974). Grain size fraction is understood in terms of processes. It varies in accordance with discharge and availability of sizes. Granulometric analysis suggests flood plain sediments are deficient in fine silt and clay with dominance of very fine sand.

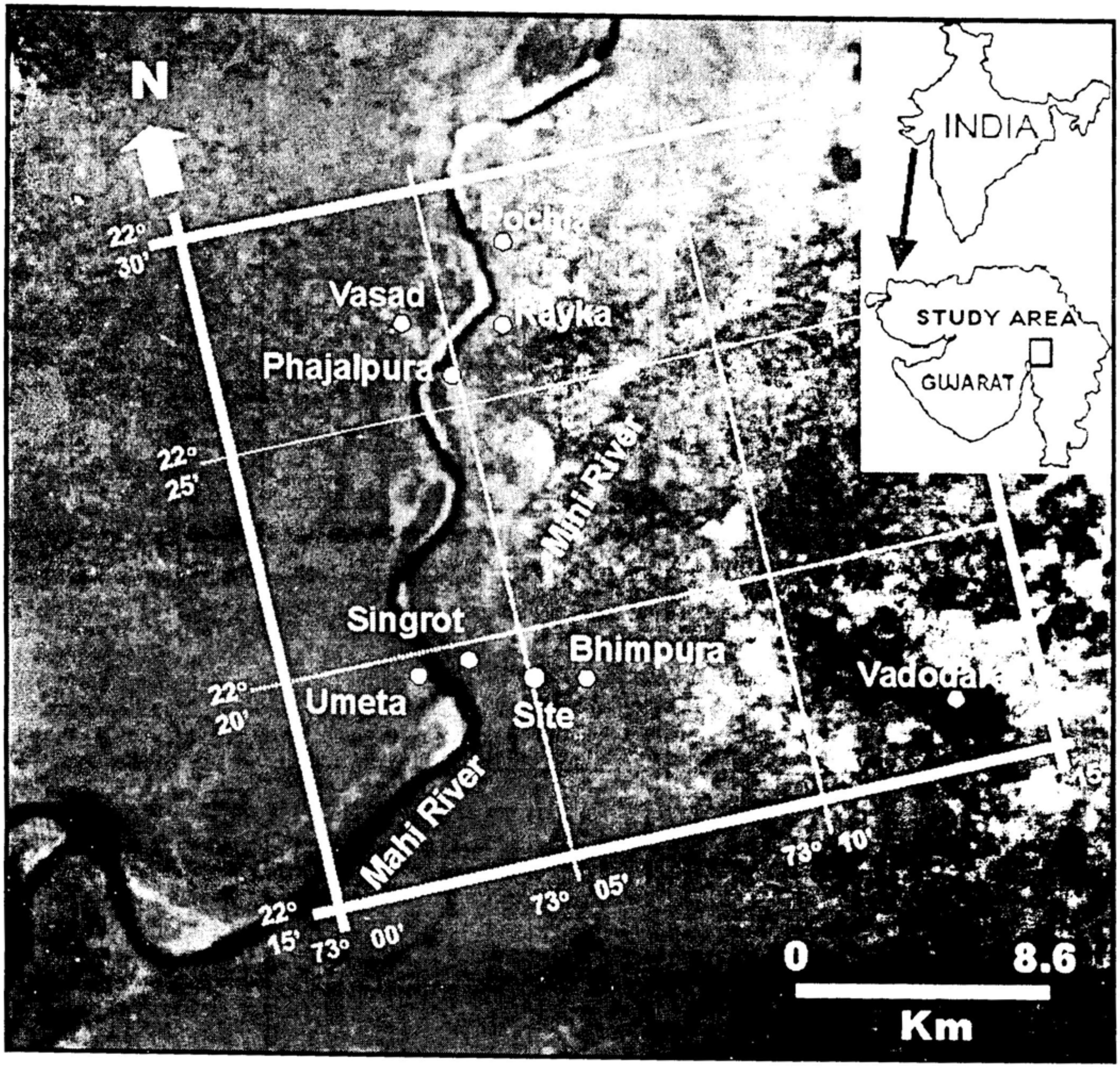

Fig. 1: Satellite image showing flood plain of river Mahi. Various important locations around Bhimpura site are shown therein

Correlation analysis among grain size fractions as well as within subgroups classified based on grain size (Folk 1974), suggests that only few grain size fractions are sensitive to change in process intensity. Such climate sensitive grain size fractions are grouped as an allogenic proxy. In the present case, grain size fractions between 210-149 μm (fine sand) and <25 μm (silt) are found to be sensitive to change in process intensity (Fig. 2). In a semi-arid, monsoonal climate, the flood plain sediment records two important processes; – *viz.* flooding and non-flooding episodes. An increase in the 210-149 μm grain size fractions represents increase in carrying capacity of a river suggesting wetter conditions. Whereas, increase in <25 μm grain size fraction represents comparatively weaker fluvial activity and mobilization and accumulation of fine sand and silt by aeolian activity suggesting a dryer climate. Based on the 210-149 μm and <25 μm grain size fractions we identify seven flooding and non flooding periods during the Last Glacial (see section 4).

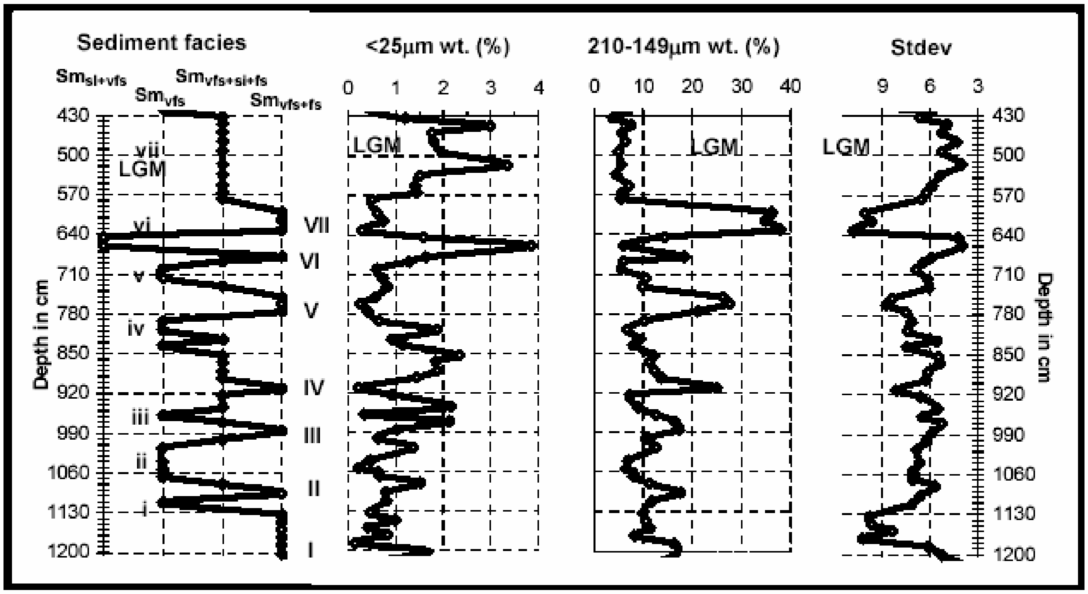

Fig. 2: Variation of sediment facies, weight percentage of <25 μm and 210-149 μm sediment fraction and standard deviation having inverse relationship with degree of sorting along the depth profile for the sediment sequence at Bhimpura site. Numbers i to vii represent non flooding event (cold and dry, stadial type) and numbers I to VII represent flooding event (warm and wet events, interstadial type) Event vii (last stadial) represent Last Glacial Maxima whereas event VII (last interstadial) represent last pre-Holocene fluvial event

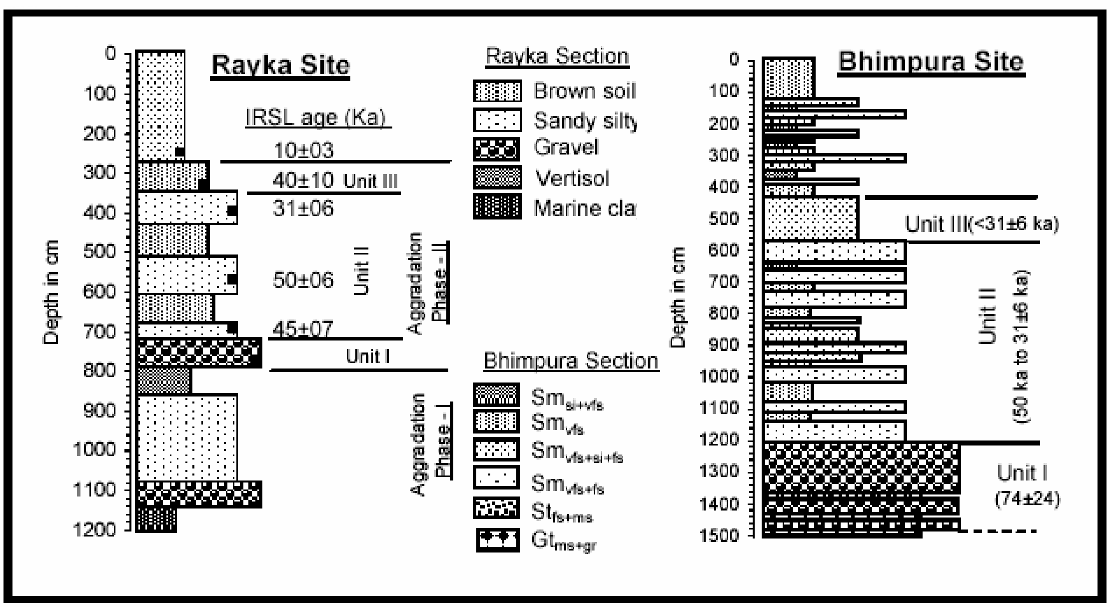

Fig. 3: Comparison of sediment facies and marker horizons for the sequence at Rayka and Bhimpura sites

Standard deviation (Stdev) of the grain size fractions captures the degree of sediment sorting. Increase in standard deviation indicates decrease in degree of sorting and vice versa. The degree of sorting when seen against the depth profile indicates that the sediments during flooding periods are relatively less sorted than sediments deposited during non-flooding events (Fig. 2). Variation in the degree of sorting along the depth correlates directly with 210-149 μm grain size fractions and inversely with <25 μm grain size fraction, thereby suggesting that the degree of sorting is a proxy for the fluctuation of energy conditions during transport and deposition. Thus, variability in degree of sorting is understood here as being sensitive to climate changes.

Cluster analysis and field characters are used to determine the facies type. Six sedimentary facies have been identified for the floodplain sequence at Bhimpura from a total depth of 1513 cm (Figs. 2-3). They are (i) trough cross-stratified gravel + medium grain sand facies (Gt) (16 samples analysed: 78% gravel + coarse to medium sand, 16% fine sand; 5% very fine sand and 1% silt), (ii) Trough cross-stratified medium sand + fine sand facies (St_{ms+fs}). (6 samples analysed: 73% medium sand, 21% fine sand, 5% very fine sand and 1% silt);
(iii) Massive unstratified very fine sand + fine sand (Sm_{vfs+fs}) (16 samples analysed: 48% very fine sand, 42% fine sand and 10% silt); (iv) Massive unstratified very fine sand + silt + fine sand ($Sm_{vfs+si+fs}$) (22 samples analysed: 61% very fine sand, 18% fine sand and 21% silt);
(v) Massive unstratified very fine sand (Sm_{vfs}) (30 samples analysed: 73% of very fine sand 14% fine sand and 13% silt) and (vi) Massive, unstratified silt + very fine sand (Sm_{vfs+si}) (7 samples analysed: 59% very fine sand, 30% silt and 11% fine sand).

The intercalated sequence of Gt and St_{ms+fs} facies forms the base of the flood plain sequence from a depth 1513 cm to 1203 cm (Fig. 3). This 310 cm thick sediment is poorly sorted. The bulk sediment comprises of gravel size clasts of calcrete and basalt supported by medium-fine grained sand. Gt and St both show trough cross-stratification, that dips 15-17° due east. Calcrete grains are of various shapes and sizes. The maximum elongation of calcrete clasts observed is 18 cm. Rhyzoliths are well developed within St_{ms+fs}. Rhyzoliths have a maximum diameter of 8 mm. Gt and St_{ms+fs} facies occurs laterally within and across the Mahi basin as the base of massive unstratified silty sandy sediments. Gt and St_{ms+fs} facies reflect a very strong fluvial regime possibly during the late Last Interglacial.

The massive unstratified silty sandy sediments show intercalation of Sm_{vfs+fs} facies with Sm_{vfs+si} – Sm_{vfs} – $Sm_{vfs+si+fs}$ facies, from depth 1203 cm to 580 cm (Figs. 2 and 3). Sm_{vfs+fs} facies are deposited with a flat base, capped or underlaid by a sharp contact with Sm_{vfs+si} – Sm_{vfs} – $Sm_{vfs+si+fs}$ facies sub-units, suggesting a heterogeneous amalgamation of sediment facies. Sm_{vfs+fs} facies shows increase in 149 μm grain size fraction, decrease in <25 μm grain size fraction and degree of sorting suggesting a channel sheet deposit of a shallow flooding river. The Sm_{vfs+si} – Sm_{vfs} – $Sm_{vfs+si+fs}$ facies shows overall increase in <25 μm grain size, decrease in 210-149 μm grain size and have a relatively moderate to low degree of sorting (Figs. 2 and 3). Sm_{vfs+fs} facies represent fluvial process whereas Sm_{vfs+si} – Sm_{vfs} – $Sm_{vfs+si+fs}$ facies represent fluvio-aeolian processes.

The sediment from 580 cm to 433 cm includes 147 cm of uniform $Sm_{vfs+si+fs}$ facies capping the last extreme flooding period (Event VII: Figs 2 and 3) marked by Sm_{vfs+fs} facies. Development of uniform $Sm_{vfs+si+fs}$ facies suggests dominance of a single process. $Sm_{vfs+si+fs}$ facies show an increase in <25 μm, flattening of 210-149 μm and increase in degree of sorting. $Sm_{vfs+si+fs}$ facies suggests strong aeolian activity in the region during non-flooding periods (Event vii: Figs. 2-3).

In summary, the presence of dune fields within the Mahi and Sabarmati flood basins suggests the role of strong winds and/or low vegetation cover in redistributing available fine sediment within and across the flood plains. Thus four allogenic proxies namely 210-149 μm and <25 μm grain size fractions, standard deviation and sediment facies are identified as climate sensitive (Fig. 2). Seven flooding and non-flooding periods have been identified at the Bhimpura site.

Opaque magnetic heavy mineral records

Opaque, magnetic minerals are separated using a hand magnet taking ten grams of bulk sample. Such separation is the initial step for preparing samples before running the sample through a Frantz Magnetic Separator, as such minerals adhere to pole pieces and interfere with flowing tracks (Hess 1966). Each magnetic fraction is weighed and finally converted to its weight percentage. This method was repeated until all Opaque magnetic heavy minerals were separated. For further confirmation, the procedure for a few samples was repeated ten times. The results show a repeatability of up to 98%.

Given the same sediment provenance of the streams an increase or decrease in opaque mineral concentration reflects intensity of transport process. The heaviness of Opaque magnetic heavy mineral causes them to travel along with medium to fine grain sediments in accordance with the relationship between specific gravity and grain size (Folk 1974; Friedman and Sanders 1978). Increase in the Opaque magnetic heavy mineral concentration is suggestive of higher energy conditions. Hence, identification of flood events can be done by observing increase in

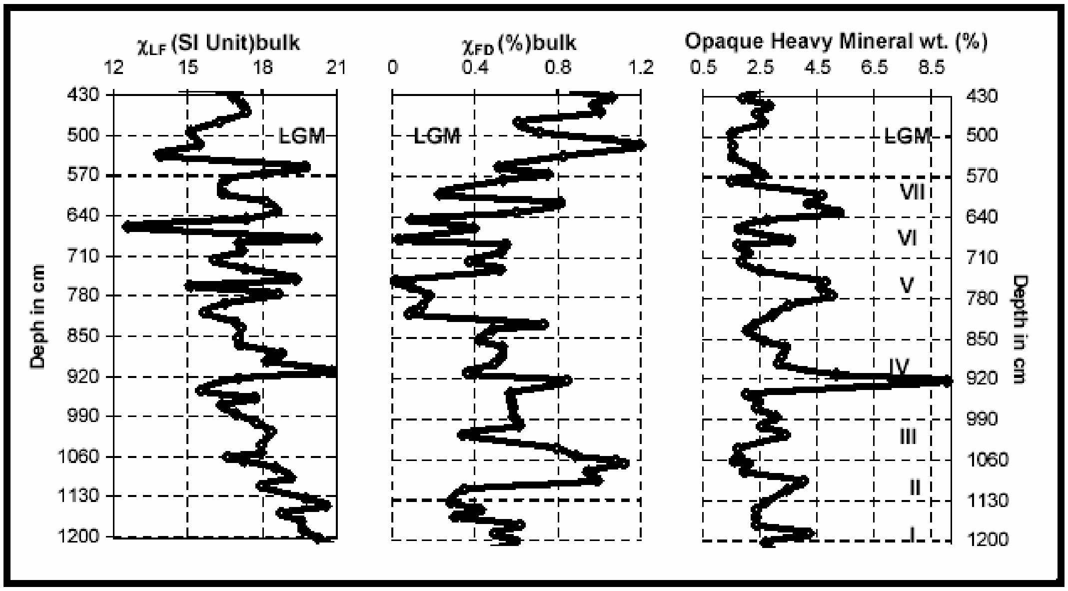

Fig. 4: Variation of Magnetic susceptibility and Opaque magnetic heavy mineral percentage along depth profile for the sediment sequence at Bhimpura site

ferromagnetic mineral concentration (Fig. 4). It was observed that an increase in Opaque magnetic heavy mineral concentration occurred with increase in the 210-149 μm grain size fraction, thus justifying seven flood periods (Figs. 2 and 4).

Magnetic susceptibility records

Magnetic susceptibility studies of Chinese loess suggest that low frequency mass susceptibility (χ_{LF}), reflects high-grade pedogenesis whereas frequency dependent magnetic susceptibility (χ_{FD}(%)) records low grade weathering (Heller *et al.* 1991; Guo *et al.* 2000). In the flood plain sediment both allogenic and authigenic processes (pedogenesis and early diagenesis of flood plain sediments) occur together. To differentiate authigenic signatures from allogenic we compare magnetic susceptibility records with Opaque magnetic heavy mineral percentages. Fig. 4 shows increase in χ_{LF}bulk indicating an increase in Opaque magnetic heavy mineral concentration. An increase in χ_{FD}(%)bulk with a decrease in Opaque magnetic heavy mineral captures pedogenesis. χ_{FD}(%) bulk captures secondary enrichment of ferrous/ferric iron due to pedogenesis. Further, χ_{LF}bulk and χ_{FD}(%)bulk record shows an inverse relationship (Fig. 4). Four pedogenic horizons identified based on χ_{FD}(%)bulk are at depths 1040 cm to 1096 cm, 825 cm, 732 cm to 687.5 cm, 577 cm to 430 cm. Each pedogenic horizons was developed within Sm_{vfs} facies just above the fluvial sand. In the field, one can identify them as a moderate pedogenic horizon as it has not attained a definite palaeosol status.

Carbonate records

Variation of carbonates (calcrete, $CaCO_3$ and calcite) signifies understanding of authigenic processes. Andrews and others (Andrews *et al.* 1998), describe calcrete carbonate formation in a monsoon setting. Calcrete precipitation takes place after the rainy season (after July to August in modern SwIM) by downward leaching of soluble $CaCO_3$ and its accumulation at the evapotranspiration front (Courty *et al.* 1987). Thus, October to March is the probable time for the formation of these Indian calcretes. Another possibility is that calcrete is a result of surface evaporation of water. Increased evaporation is also likely to be an indicator of a more arid environment.

Carbonate percentage from depth 1133 to 880 cm increases from 18% to 63%, and thereafter fluctuates between 30-45%. Nevertheless, the calcrete and calcite percentages show a positive relation with <25 μm grain size fraction and at the same time an inverse relation with 210-149 μm grain size fraction, sediment facies and Opaque magnetic heavy mineral percentage (Figs. 2, 4, and 5). Based on percentages of calcrete and calcite, we are able to distinguish five horizons at depths; 1096 cm to 1016 cm, 985 cm to 911 cm, 880cm to 825 cm, 732 cm to 687 cm, and 577 cm to 430 cm. These represent periods of relatively more aridity (Fig. 5).

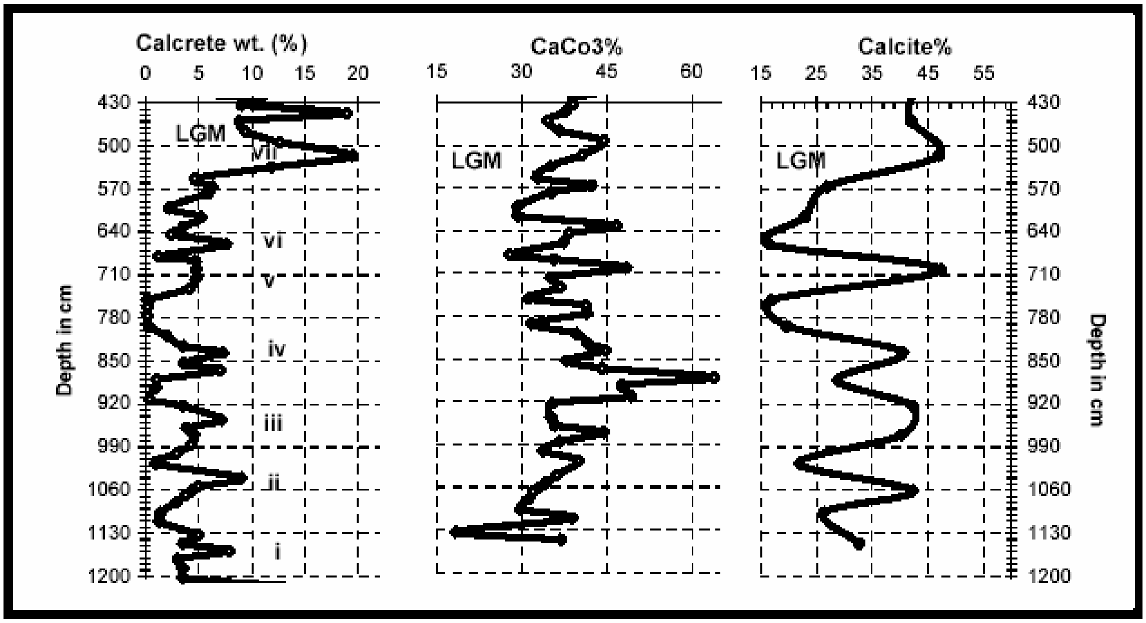

Fig. 5: Variation of Carbonates percentage (calcrete carbonate, $CaCO_3$ and mineral calcite) along the depth profile for the sediment sequence at Bhimpura site

Mineralogical records

Composition of sediment is determined from the assemblage of common rock forming minerals (quartz and feldspar), clay minerals (smectite, chlorite, illite) and other secondary minerals (calcite and hematite). Quartz and feldspars (sp. gr. 2.65-2.76) either reflect an increase or decrease in sediment discharge. Clay minerals within the sediment would represent both allogenic and authogenic transformations. Allogenic component is understood with increase or decrease of clay minerals depending on fractionation based on their density, smectite 2-2.6 gm/cc (lowest density); Illite 2.6-2.9 gm/cc; chlorites 2.6-3.3 gm/cc (highest density) (Deer *et al.* 1966 as cited in Totten *et al.* 2002).

It is possible to infer that in the zone where calcrete is enriched, the percentage of smectite increases while the illite percentage decreases. This is due to alteration of illite under alkaline conditions. There is a distinct change in the mineral percentages from a depth of 640 cm upwards. Quartz and feldspars decreases, illite percentages follow the same trend whereas smectite increases. Therefore, mineral percentages indicate a major change in the type of depositional processes (Fig. 6), which can be correlated with climatic signatures deduced from the aforesaid parameters. In a clay-silt deficient flood plain sediment, the concentration of clay minerals (smectite, illite and chlorites), however small are significant.

Age Bracket of the Sedimentary Sequence

Variation in sedimentary facies along a depth profile for Rayka and Bhimpura sites are recorded in Fig. 3. Vertisol (10 YR 7/4, very pale brown) forms the base of the sequence. At Rayka sites, vertisol is well documented whereas at the Bhimpura site, the presence of vertisol is inferred to extend below Gt and St_{ms+fs} facies based on neighboring sections. The vertisol is overlain by Gt and St_{ms+fs} facies (10 YR 6/4, light yellowish brown) at Rayka and Bhimpura. We identify this as Unit I. Unit II, immediately overlying Unit I, comprises intercalated Sm_{vfs+fs} facies (10 YR 7/6, yellow) and Sm_{vfs+si} – Sm_{vfs} – $Sm_{vfs+si+fs}$ facies (10 YR 6/6, brownish yellow) sequence at Rayka and Bhimpura sites. Finally, the sequence is capped by a thick pedogensied $Sm_{vfs+si+fs}$ facies (10YR 7/6, yellow) is identified as Unit III.

Both the sections, Rayka and Bhimpura, show three significant marker horizons based on sediment characteristics (Figs. 2 and 3). The first marker is Unit I. The second marker is the sandy facies immediately overlaying Unit I at Rayka and Bhimpura. The upper most portion of Unit II with sandy facies forms the third marker (Rayka, 476 cm to 400 cm; Bhimpura, 659 cm to 577 cm). The third marker is immediatly overlain by a pedogensied sandy silt facies along various sections within the Mahi basin. The lateral extension of all these markers has been traced throughout the study area.

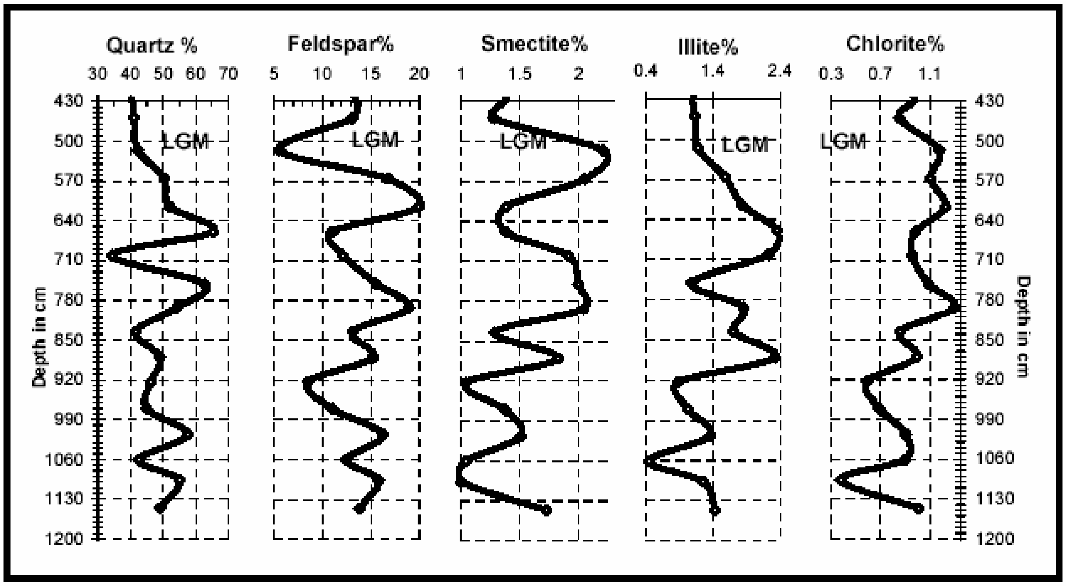

Fig. 6: Variation of common rock forming and clay minerals in percentages along the depth profile for the sediment sequence at Bhimpura site

The chronological data for the Rayka section suggests that the age of the first marker is 74±24 ka. The second marker is dated to about 50 ka (between 50±6 ka and 45±7 ka) while the third marker is dated to 31±6 ka. (Juyal *et al.* 2000). Therefore the age of Unit I falls around 74±24 ka whereas Unit II spans a period ranging from 50 ka to 31±6 ka. Unit III fall around <31±6 ka. Thus, the flood plain most of the sequence spans over most of the Last Glacial.

Climate Change: A Synthesis

The identification of short-term climatic episodes (flooding and non-flooding episodes) from the Bhimpura flood plain sediments, is based on climate sensitive parameters in flood plain deposits discussed above. In all, seven flooding and non-flooding episodes are identified based on these parameters from depths of 433 cm to 1202 cm. The 769 cm thick intercalated sedimentary sequence (Sm_{vfs+fs} facies intercalates within Sm_{vfs} – $Sm_{vfs+si+fs}$ – Sm_{si+vfs} facies) spans the Last Glacial.

Flooding episodes (I to VII) are characterized by Sm_{vfs+fs} facies. Increase in 210-149 μm grain size fraction, Opaque magnetic heavy mineral percentages and decrease in degree of sorting, and χ_{LF}bulk characterizes flooding episodes (Figs. 2 and 4). The behaviour of these climate sensitive parameters suggests that these episodes had a relatively high sediment carrying capacity. Based on this, it is inferred that during these periods, torrential rains led to flash floods in the shallow river channels (Ice Age rivers). The transitory, short-lived rivers during the Last Glacial were dependent entirely on the SwIM leading to rapid denudation.

Non-flood episodes (i to vii) are characterized by Sm_{vfs} – $Sm_{vfs+si+fs}$ – Sm_{si+vfs} facies. Increase in the <25 μm grain size fraction, degree of sorting, χ_{FD}bulk, and calcrete percentages along with a decrease in Opaque magnetic heavy mineral, quartz and feldspar percentages (Figs 2, 4, 5 and 6) characterize non flooding episodes. Variation in the concentration of the said parameters suggests a feeble carrying capacity of these rivers. It further suggests that during a non-flooding climate phase, rivers were sluggish, with reduced erosion. Reduction and prolongation of the SwIM would increase the rate of evaporation, and decrease vegetation cover, initiating reworking of moisture free sediments by strong winds. This additional process within the flood plain resulted in development of sheets and dunes. The increase in <25 μm grain size fraction, degree of sorting, χ_{FD}bulk, and calcrete percentages supports this view (Figs. 2, 4-5).

Moreover, during non-flood episodes, there is a decrease in precipitation, which influences the chemistry of ground water leading to authigenic changes. The role of authigenic processes in the sediments is represented by percentages of carbonate, calcrete carbonates and calcite (Fig. 5). One of the important authigenic activities in monsoonal setting is the result of downward leaching of soluble $CaCO_3$ or surface evaporation. We observe increase in calcrete carbonate and calcite during non flood episodes correlated with the quantity of the <25 μm grain size fraction. Further an alkaline environment during non-flood episodes seems to have allowed transformation of illite to smectite (Fig. 6). Clay minerals such as smectite, illite, and chlorite reflect a significant change between 640 cm to 570 cm (Fig. 6).

Thus, the present allogenic and authigenic records from the flood plain sediment significantly contributes to characterizing both flooding as well as non-flooding episodes. These events directly point towards variations in the SwIM intensity over the scale of a few thousand years during the Last Glacial that led to aggradation and avulsion.

Analysis of ice cores (Polar: Jouzel *et al.* 1987; Greenland ice core project members 1993; Grootes *et al.* 1993; Dansgaard *et al.* 1993) and ocean core sediments (Atlantic and Indian Ocean: Ruddiman 1977; Bond *et al.* 1992; Grousset *et al.* 1993; Schulz *et al.* 1998; Colin *et al.* 1998; Heinrich 1988; Leuschner and Sirocko 2000; Altabet *et al.* 2002) have also revealed that climate fluctuated during the Last Glacial, evidence of which is preserved as abrupt climatic events. These short-term, warm and wet climatic events (interstadials) are globally expressed in terms of Dansgaard-Oeschger (D/O) events, which culminated with relatively long term dry-cool cycles (stadials) called Heinrich events (Ruddiman 1977; Heinrich 1988; Bond *et al.* 1992; Dansgaard *et al.* 1993; Grousset *et al.* 1993). In China and Central Asia, these short-term abrupt climatic events are identified, on the basis of studies on grain sizes of loess sediments(Porter and An 1995; Porter 2001). The coarsening of grain size in Chinese loessic sediments is inferred as representing the Heinrich event. The mechanism suggested to explain this process is increase in continental wind speed and aridity. Further, it is also observed that the type of fluctuations in grain size (which is a proxy to river discharge and on-land weathering processes) of sediments in the Bay of Bengal – Andaman sea (site MD77-169 and MD77-180) is comparable with D/O type fluctuations. These fluctuations indicate an increased summer monsoon during D/O, and significantly drier conditions during Heinrich events (Colin *et al.* 1998). The D/O variability of the Indian monsoon is also revealed in the Arabian Sea record (site 93KL: Schulz *et al.* 1998).

In the light of these observations, flood episodes deduced from the Bhimpura site could be interpreted as being under the direct influence of D/O type fluctuations. High-resolution climate sensitive proxies and chronology for flood plain sediments would further confirm continental response to such abrupt events.

Acknowledgments

This work was supported in part by a grant from the Department of Science and Technology, India. DAS would like to thank the Nonlinear Studies Group, Indian Institute of Science, Bangalore for support. GR is associated with the Jawaharlal Nehru Centre for Advanced Scientific Research as a Honorary Faculty Member. GR was also supported by the Homi Bhabha Fellowship and DRDO, India. The authors would like to thank Prof. S.N. Rajaguru and Dr. V. Purnachandra Rao for helping us during various stages of the work. We thank Prof. Vishwas S. Kale, University of Poona and Prof. Ravi Korisettar, Karnataka University for critically reviewing the manuscript. We further thank Prof. R.J. Wasson, Canberra Australia for critical review and suggestions to improve the manuscript.

References

Allchin, B. and A.Goudie 1971. Dunes, Aridity and Early Man in Gujarat, Western India, *Man* 6: 248-265.

Allchin, B., A.Goudie and K.T.M. Hegde 1978. *The Prehistory and Palaeogeography of the Great Indian Desert*. London: Academic Press.

Altabet, M.A., M.J. Higginson and D.W. Murray 2002. The Effect of Millennial-Scale Changes in Arabian Sea Denitrification on Atmospheric CO_2. *Nature* 415: 159-162.

Andrews, J.E., A.K. Singhvi, A.J. Kailath, R. Kuhn, P.F. Dennis, S.K. Tandon and R.P. Dhir 1998. Do Stable Isotope Data from Calcrete Record Late Pleistocene Monsoon Climate Variation in the Thar Desert of India? *Quaternary Research* 50: 240-251.

Bond, G., H. Heinrich, W. Broecker, L. Labeyrie, J. McManus, J. Andrews, S. Huon, R. Jantschik, S. Clasen, C. Simet, K. Tedesco, M. Klas, G. Bonani and S. Ivy 1992. Evidence for Massive Discharge of Iceberg into North Atlantic Ocean During the Last Glacial Period, *Nature* 360: 245-249.

Bonnefille, R. and F. Chalié 2000. Pollen-inferred Precipitation Time-series from Equatorial Mountains, Africa, the Last 40 kyr BP, *Global and Planetary Change* 26(1-3): 25-50.

Castelltort, S. and J.V. Driessche 2003. How Plausible are High Frequency Sediment Supply-driven Cycles in the Stratigraphic Record?, *Sedimentary Geology* 157: 3-13.

Chamyal, L.S. and S.S. Merh 1992. Sequence Stratigraphy of the Surface Quaternary Deposits in the Semi-arid Basin of Gujarat, *Man and Environment* 17: 33-40.

Colin, C., C. Kissel, D. Blamart and L. Turpin 1998. Magnetic Properties of Sediments in the Bay of Bengal and the Andaman Sea: Impact of Rapid North Atlantic Ocean Events on the Strength of the Indian Monsoon, *Earth and Planetary Science Letters* 160: 623-635.

Courty, M.A., R.P. Dhir and H. Raghavan 1987. Microfabric of Calcium Carbonate Accumulation in Arid Soils of Western India, in *Micromorphologie des Sols* (M. Fedoroff and M. A. Courty Eds.) pp. 227-234. Association Francaise pour l'Etude du sol.

Dansgaard, W., S.J. Johnsen, H.B. Clausen, D. Dahl-Jensen, N.S. Gundestrup, C.U. Hammer, C.S. Hvidberg, J.P. Steffensen, A.E. Sveinsbjörnsdottir, J. Jouzel and G. Bond 1993. Evidence for General Instability of Past Climate from a 250- kyr Ice-core Record, *Nature* 364: 218-220.

Enzel, Y., L.L. Ely, S. Mishra, R. Ramesh, R. Amit, B. Lazar, S.N. Rajaguru, V.R. Baker and A. Sandler 1999. High Resolution Holocene Environmental Changes in Thar Desert, Northwestern India, *Science* 284: 125-128

Folk, R.L 1974. *Petrology of Sedimentary Rocks*. Texas: Hemphill Publishing Co. Drawer M. University Station Austin.

Friedman, G.M. and J.E. Sanders 1978. *Principles of Sedimentology*. New York: John Wiley and Sons.

Gasse, F. and E. Van Campo 1998. A 40,000 yr Pollen and Diatom Record from Lake Tritrivakely Madagascar, in the Southern Tropics, *Quaternary Research* 49: 299-311.

Greenland Ice-core Project Members 1993. Climate Instability During the Last Interglacial Period Recorded in the GRIP Ice Core, *Nature* 364: 203-207.

Grootes, P.N., M. Stuiver, J.W.C. White, S. Johnson J. Jouzel 1993. Comparison of Oxygen Isotope Records from the GISP2 and GRIP Greenland Ice Cores, *Nature* 366: 552-554.

Grousset, F.E., L. Labeyrie, J.A. Sinko, M. Cremer, G. Bond, J. Duprat, E. Cortijo and S. Huon 1993. Patterns of Ice-rafted Detritus in the Glacial North Atlantic (40-55°N), *Paleoceanography* 8: 175-192.

Guo, Z., P. Biscaye, L. Wei, X. Chen, S. Peng and T. Liu, 2000. Summer Monsoon Variation over the last 1.2 Ma from the Weathering of Loess-soil Sequence in China, *Geophysical Research Letters* 27(12): 1751-1754.

Gupta, A.K. and E. Thomas 2003. Initiation of Northern Hemisphere Glaciation and Strengthening of the Northeast Indian Monsoon: Ocean Drilling Program Site 758 Eastern Equatorial Pacific, Geology 31: 47-50.

Heinrich, H. 1988. Origin and Consequences of Cyclic Ice Rafting in the Northeast Atlantic Ocean During the Past 130,000 Years, *Quaternary Research* 29: 142-152.

Heller, F., H.Y. Liu, T.S. Liu and T. Xu 1991. Magnetic Susceptibility of Loess in China. *Earth and Planetary Science Letters* 103: 301-310.

Jain, M. and S.K. Tandon 2003. Quaternary Alluvial Stratigraphy and Palaeoclimatic Reconstruction at the Thar Margin, *Current Science* 84(8): 1048-1055.

Jouzel, J., C.Lorius, J.R. Petit, C. Genthon, N.I. Barkov, V.M. Kotlyakov and V.M. Petrov 1987. Vostok Ice Core: A Continuous Isotope Temperature Record over the Last Climate Cycle (160, 000 years), *Nature* 329: 403-408.

Juyal, N., R. Raj, D.M. Maurya, L.S. Chamyal and A.K. Singhvi 2000. Chronology of Late Pleistocene Environmental Changes in the Lower Mahi Basin, Western India. *Journal of Quaternary Science* 15: 501-508.

Juyal, N., L.S. Chamyal, S. Bhandari, D.M. Maurya and A.K. Singhvi 2004. Environmental Changes during Late Pleistocene in the Orsang River Basin, Western India, *Journal of the Geological Society of India* 64(4): 417-479.

Juyal, N., A. Kar, S.N. Rajaguru and A.K. Singhvi 2003. Luminescene Chronology of Aeolian Deposition during the Late Quaternary on the Southern Margin of Thar Desert, India, *Quaternary International* 104: 87-98.

Kale, V.S., A. Gupta and A.K. Singhvi 2004. Late Pleistocene-Holocene Palaeohydrology of Monsoon Asia, *Journal of the Geological Society of India* 64(4): 403-417.

Khadkikar, A.S., G. Mathew, J.N. Malik, T.K. Gundu Rao, M.P. Chowgaonkar and S.S. Merh 1999. The Influence of the South-west Indian Monsoon on Continental Depositional over past 130Kyr, Gujarat, Western India. *Terra Nova* 11: 273-277.

Knox, J.C. 2000. Sensitivity of Modern Floods to Climate Change, *Quaternary Science Review* 9: 439-457.

Kohfeld, K.E. 2001. Late Quaternary Aeolian Deposition on the Chinese Loess Plateau, in MPI-BGC Technical Report-3 (K.E. Kohfeld and S.P. Harrison Eds.) pp. 23-26.

Kotlia, B.S., M.S. Bhalla, C. Sharma, G. Gopalan, R. Ramesh, M.S. Chauhan, P.D. Mathur, S. Bhandari, C.T. Chacko 1997. Palaeoclimatic Conditions in Upper Pleistocene and Holocene Bhimtal-Nukuchiatal Basin in South Central Kuman, India, *Palaeogeography, Palaeoclimatology, Palaeoecology* 130: 307-322.

Leuschner, D.C. and F. Sirocko 2000. The Low-latitude Climate during Dansgaard-Oeschger Cycles and Heinrich Events, *Quaternary Science Review* 19: 243-354.

Macklin, M.G. and J. Lewin 2003. River Sediment, Great Floods and Centennial-scale Holocene Climate Change, Journal of Quaternary Science 18(2): 101-105.

Malik, J.N., A.S. Khadkikar and S.S. Merh 1999. Allogenic Control on Late Quaternary Continental Sedimentation in the Mahi River Basin, Western India, *Journal of the Geological Society of India* 53: 299-314.

Merh, S.S. and L.S. Chamyal 1997. The Quaternary Geology of the Gujarat Alluvial Plain, *Proceedings of the Indian National Science Academy* 63A: 1-98.

Mishra, S. and S.N. Rajaguru 2001. Late Quaternary Palaeoclimate of Western India: A Geoarchaeological Approach, *Mausam* 52: 285-296.

Overpeck, J., D. Anderson, S. Trumbore and W. Prell 1996. The Southwest Indian Monsoon over last 18,000 years, *Climate Dynamics* 12:`213-225.

Pant, R.K. and L.S. Chamyal 1990. Quaternary Sediment Pattern and Terrain Evolution in the Mahi River Basin, Gujarat, India, *Proceedings of Indian National Science Academy* 56: 501-511.

Porter, S.C. 2001. Chinese Loess Record of Monsoon Climate during the Last Glacial-interglacial Cycle, *Earth Science Review* 54: 115-128.

Porter, S.C. and Z. An 1995. Correlation between Climatic Events in North Atlantic and China during Last Glaciation, *Nature* 375: 305-308.

Rangarajan, G. and D.A. Sant 2000. Paleoclimatic Data from 74KL and Guliya Cores: New Insight, *Geophysical Research Letters* 27: 787-790.

Ruddiman ,W.F. 1977. Late Quaternary Deposition of Ice-rafted Sand in the Subpolar North Atlantic (lat 40° and 65°N), *Geological Society of America Bulletin* 88: 1813-1827.

Sant, D.A. and R.V. Karanth 1993. Drainage Evolution of the Lower Narmada Valley, Western India, *Geomorphology* 8: 221-244.

Sant, D.A., K. Krishnan, G. Rangrajan, N. Basaviah, C. Pandya, M. Sharma and Y. Trivedi 2004. Characterization of Flood Plain and Climate Change using Proxies Records from the Mahi River Basin Mainland Gujarat, *Journal of Indian Geophysical Union* 8(1): 39-48.

Sant, D.A. and G. Rangarajan 2002. Onset of Climate at Last Glacial-Holocene Transition: Role of the Tropical Pacific, *Current Science* 83: 1398-1402.

Sarkar, A., R. Ramesh, B.L.K. Somayajulu, R. Agnihotri, A.T. Jull and G.S. Burr 2000. High Resolution Holocene Paleomonsoon Record from the Eastern Arabian Sea. *Earth Planetary Science Letters* 177(3-4): 209-218.

Schulz, H., U. von Rad and H. Erlenkeuser 1998. Correlation between Arabian Sea and Greenland Climate Oscillations of the Past 110,000 Years, *Nature* 393: 54-57.

Singh, I.B. 2004. Late Quaternary History of the Ganga Plain, *Journal of the Geological Society of India* 64(4): 431-454.

Sinha, R., D. Stueben and Z. Berner 2004. Palaeohydrology of the Sambhar Playa, Thar Desert, India using Geomorphology and Sedimentological Evidences, *Journal of the Geological Society of India* 64(4): 419-430.

Sirocko, F., M. Sarnthein, H. Erlenkeuser, H. Lange, M. Arnold and J.C. Duplessy 1993. Century-scale Events in Monsoonal Climate over Past 24,000 Years, *Nature* 354: 322-324.

Srivastava, P., N. Juyal, A.K. Singhvi, R.J. Wasson and M.D. Bateman 2001 Luminescence Chronology of River Adjustment and Incision of Quaternary Sediment in the Alluvial Plain of the Sabarmati River, North Gujarat, India, *Geomorphology* 36: 217- 229.

Subbarao, B. 1952. Archaeological Explorations in Mahi Valley, *Journal of Maharaja Sayajirao University of Baroda* 1: 33-74.

Tandon, S.K., B.K. Sareen, M.S. Rao and A.K. Singhvi 1997. Aggradation History and Luminescence Chronology of Late Quaternary Semi-arid Sequence of the Sabarmati Basin, Gujarat, Western India, *Palaeogeography, Palaeoclimatology, Palaeoecology* 128: 339-357.

Thamban, M., P.V. Rao, R.R. Schneider, P.M. Grootes 2001. Glacial to Holocene Fluctuations in Hydrography and Productivity along the Southwestern Continental Margin of India, *Palaeogeography, Palaeoclimatology, Palaeoecology* 165: 113-127.

Thompson, L.G., T. Yao, M.E. Davis, K.A. Henderson, E.M. Thompson, P.N.Lin, J. Beer, H.A. Synal, J. Cole-Dai and J.F. Bolzan 1997. Tropical Climate Instability: The Last Glacial Cycle from a Qinghai-Tibetan Ice Core, *Science* 276: 1757-1825.

Tooth, S. 2000. Process, form and change in dryland rivers: a review of recent research. *Earth-science Reviews* 51: 67-107.

Totten, M.W., M.A. Hanan, D. Knight and J. Borges 2002. Characteristics of Mixed-Layer Smectite/illite Density Separates during Burial Diagenesis, *American Mineralogist* 87: 1571-1579.

Wang, L.J., X.L. Wang, M. Sarnthein, P.M. Grootes, H. Erlenkeuser and P. Wang 1999. Millennial Reoccurrence of Century-scale Abrupt Events of East Asian Monsoon: A Possible Heat Conveyor for the Global Deglaciation, *Paleoceanography* 14: 725-731.

Wasson, R.J., S.N. Rajaguru, V.N. Mishra, D.P. Agrawal, R.P. Singh, A.K. Singhvi, and K. Kameswar Rao 1983. Geomorphology, Late Quaternary Stratigraphy and Palaeoclimatology of the Thar Dune Field, *Zeitschrift für Geomorphologie* 45: 117-151.

Xiao, J., S.C. Porter, Z. An, H. Kumai and S. Yoshikawa 1995. Grain Size of Quartz as an Indicator of Winter Monsoon Strength on the Loess Plateau of Central China during the Last 130,000Yr. *Quaternary Research* 43: 22-29.

Zeuner, F.E.1950. *Stone Age and Pleistocene Chronology in Gujarat,* Pune: Deccan College.